INTERNATIONAL CENTRE FOR THEORETICAL PHYSICS
94/2111
2 8 APR 1994
LIBRARY

IC/94/71

INTERNATIONAL CENTRE FOR THEORETICAL PHYSICS

A HYBRID METHOD FOR THE ESTIMATION OF GROUND MOTION IN SEDIMENTARY BASINS: QUANTITATIVE MODELLING FOR MEXICO CITY

D. Fäh

P. Suhadolc

St. Mueller

and

G. F. Panza

INTERNATIONAL ATOMIC ENERGY AGENCY

UNITED NATIONS EDUCATIONAL, SCIENTIFIC AND CULTURAL ORGANIZATION

MIRAMARE-TRIESTE

IC/94/71

International Atomic Energy Agency
and
United Nations Educational Scientific and Cultural Organization
INTERNATIONAL CENTRE FOR THEORETICAL PHYSICS

A HYBRID METHOD FOR THE ESTIMATION OF GROUND MOTION IN SEDIMENTARY BASINS: QUANTITATIVE MODELLING FOR MEXICO CITY

Donat Fäh
Istituto di Geodesia e Geofisica, Università degli Studi di Trieste,
via dell'Università 7, 34124 Trieste, Italy
and
Institut für Geophysik, ETH Hönggerberg, CH-8093 Zürich, Switzerland,

Peter Suhadolc
Istituto di Geodesia e Geofisica, Università degli Studi di Trieste,
via dell'Università 7, 34124 Trieste, Italy,

Stephan Mueller
Institut für Geophysik, ETH Hönggerberg, CH-8093 Zürich, Switzerland

and

G.F. Panza
International Centre for Theoretical Physics, Trieste, Italy
and
Istituto di Geodesia e Geofisica, Università degli Studi di Trieste,
via dell'Università 7, 34124 Trieste, Italy.

MIRAMARE - TRIESTE
April 1994

Abstract

To estimate the ground motion in two-dimensional, laterally heterogeneous, anelastic media, a hybrid technique has been developed which combines modal summation and the finite difference method. In the calculation of the local wavefield due to a seismic event, both for small and large epicentral distances, it is possible to take into account the source, path and local soil effects.

As practical application we have simulated the ground motion in Mexico City caused by the Michoacan earthquake of September 19, 1985. By studying the one-dimensional response of the two sedimentary layers present in Mexico City, it is possible to explain the difference in amplitudes observed between records for receivers inside and outside the lake-bed zone. These simple models show that the sedimentary cover produces the concentration of high-frequency waves (0.2-0.5 Hz) on the horizontal components of motion. The large amplitude coda of ground motion observed inside the lake-bed zone, and the spectral ratios between signals observed inside and outside the lake-bed zone can only be explained by two-dimensional models of the sedimentary basin. In such models, the ground motion is mainly controlled by the response of the uppermost clay layer. The synthetic signals explain the major characteristics (relative amplitudes, spectral ratios, and frequency content) of the observed ground motion. The large amplitude coda of the ground motion observed in the lake-bed zone can be explained as resonance effects and the excitation of local surface waves in the laterally heterogeneous clay layer. Also, for the 1985 Michoacan event, the energy contributions of the three subevents are important to explain the observed durations.

Introduction

Numerical simulations play an important role in the estimation of strong ground motion in sedimentary basins. They can provide synthetic signals for areas where recordings are absent, and are therefore very useful for engineering design of earthquake-resistant structures. In recent years many computational techniques have been proposed to estimate ground motion at a specific site. The methods commonly used are one- and two-dimensional techniques; three-dimensional studies are too expensive to be applied routinely. The standard one-dimensional methods, such as the Thomson-Haskell method (Thomson, 1950; Hakell, 1953), are very cheap and they easily provide the first few resonance frequencies (fundamental and harmonics) of unconsolidated sedimentary layers. The results show that the strongest effects usually occur at the fundamental frequency. Relative to the response of a reference, bedrock model, one-dimensional techniques yield estimates of the wave amplification caused by unconsolidated surficial sediments overlying the bedrock. However, such techniques fail to predict the ground motion close to lateral heterogeneities or when the sedimentary layers have a non-planar geometry. For realistic structures where lateral heterogeneities and sloping layers are common, these departures from lateral homogeneity can cause effects that dominate the ground motion: the excitation of local surface waves, focusing and defocusing, and spatially variable resonances. Thus the treatment of realistic structures requires at least two-dimensional techniques to estimate ground motion. In many of these techniques, such as in the finite difference (e.g. Alterman and Karal, 1968) or finite element methods (e.g. Lysmer and Drake, 1972), the source cannot be included in the structural model, because its distance from the site of interest is too large. The incoming wavefield is then approximated by a plane polarized body-wave. Other techniques, such as the 2D

mode summation method (Levshin, 1985; Vaccari et al., 1989), are capable of treating realistic source models, but can be practically applied only to simple two-dimensional geometries of sedimentary basins.

To include both a realistic source model and a complex structural model of the sedimentary basin, a hybrid method has been developed that combines modal summation and the finite difference technique (Fäh et al., 1990; Fäh, 1992). The propagation of waves from the source position to the sedimentary basin is treated with the mode summation method for a plane layered structure. Explicit finite difference schemes are then used to simulate the propagation of seismic waves in the sedimentary basin. This hybrid method is particularly suitable to estimate ground motion in sedimentary basins of any complexity, and it allows us to take into account the source, path, and local site effects, even when dealing with path lengths of a few hundred kilometers. A similar method that combines modal summation and the finite element technique has been used by Regan and Harkrider (1989) to study the propagation of SH Lg waves in and near continental margins.

Numerical simulations should always be compared with observed ground motion for the same simulated event to establish validity of the numerical results. This will be done for the case of Mexico City which has experienced extensive damage in the recent past due to strong earthquakes with hypocenters in the Mexican subduction zone. The Michoacan earthquake of September 19, 1985 (M_S=8.1), together with its aftershocks, produced the worst earthquake damage in the history of Mexico. Although the epicenter of the earthquake was close to the Pacific coastline, damage at coastal sites was relatively small. The reason for this is that most of the populated areas near the coast are situated on hard bedrock. In contrast, Mexico City, which is about 400 km away from the epicenter, suffered extensive damage. This can be

attributed to the geotechnical and geometrical characteristics of the sediments in the valley of Mexico City. They were responsible for a very long duration of ground motion with large amplitude coda, and large relative spectral amplifications which reached values of up to 50.

Using data from a recently installed VBB (Very Broad Band) seismograph at CU (a hill-zone site of Mexico City) Singh and Ordaz (1992) proposed a simple explanation of the long duration of recorded coda in the lake-bed zone. They state that the long duration coda has always been present in the excitation, but the accelerations did not reach the necessary threshold for the standard instruments at hill-zone sites to remain triggered. The clay layers present in the lake-bed zone are natural narrow-band amplifiers that expain the recorded coda. They reach the conclusion that two- or three-dimensional models are not needed to account for the duration observed in the lake-bed zone. Their conclusion is based on only indirect and qualitative comparisons: they compare observed signals and synthetics (obtained with one-dimensional modelling) for different events. Therefore, they could not give quantitative estimates of the amplification in the lake-bed zone with respect to a hill-zone site, since the hill-zone-site duration and waveform of the two earthquakes could be completely different. However, they fail to provide an explanation for the records (e.g. station CDAO) that exhibit a large amplitude coda well within the time windows for which stations on firm sites (e.g. station TACY) were recording. As was already shown by Kawase and Aki (1989), one-dimensional modelling fails to explain this effect; and spectral ratios obtained with theoretical one-dimensional models can not explain the observations. Moreover, the variability and polarization of ground motion in the lake-bed zone can also not be interpreted with one-dimensional models (F.J. Sánchez-Sesma, personal communication). These facts motivate the present-day research towards two- and three-dimensional modelling of wave propagation in sedimentary basins.

The two-dimensional numerical modelling of the Michoacan earthquake, and the effects of this earthquake in Mexico City exhibits some interesting numerical problems that arise from the large distance of Mexico City from the seismic source. This distance causes a long duration of the incident seismic signals in Mexico City, and the presence there of sediments with very low shear-wave velocities requires the use of a small grid spacing in the finite difference computations. This small grid spacing, on the other hand, requires very efficient absorbing boundaries in the finite difference part of the hybrid approach.

The hybrid method

The hybrid technique combines modal summation and the finite difference method, and it can be used to study wave propagation in sedimentary basins. Each of the two techniques is applied in that part of the structural model where it works most efficiently: the finite difference method in the laterally heterogeneous part of the structural model which contains the sedimentary basin (see Figure 1), and modal summation is applied to simulate wave propagation from the source position to the sedimentary basin of interest. The use of the mode summation method allows us to include an extended source, which can be modelled by a sum of point sources appropriately distributed in space and time. The path from the source position to the sedimentary basin can be approximated by a structure composed of flat, homogeneous layers. Modal summation then allows the treatment of many layers which can take into consideration low-velocity zones and fine details of the crustal section under consideration. The finite difference method, applied to wave propagation in the sedimentary basin, permits the modelling of wave propagation in complicated and rapidly varying velocity structures, as is required when dealing with

sedimentary basins. The coupling of the two methods is carried out by introducing the time series obtained with modal summation into the finite difference computations.

In the modal summation method, the treatment of P-SV waves is based on Schwab's (1970) optimization of Knopoff's (1964) method (Panza, 1985), and the handling of SH waves is based on Haskell's (1953) formulation (Florsch et al., 1991); these computations include the "mode-follower" procedure and structure minimization described by Panza and Suhadolc (1987). The introduction of anelasticity into the computations is based on variational methods (Takeuchi and Saito, 1972; Schwab and Knopoff, 1972), and includes Futterman's (1962) results concerning the dispersion of body-waves in a linearly anelastic medium.

The seismic source is introduced by using the Ben-Menahem and Harkrider (1964) formalism. In these expressions, the first-term approximation to cylindrical Hankel functions is used which gives the displacements in the far field. Calculation of synthetic seismograms is then accurate to at least three significant figures, as long as the distance to the source is greater than the wavelength (Panza et al., 1973). The seismograms computed with modal summation contain all the body waves and surface waves, whose phase velocities are smaller than the S-wave velocity of the half-space that terminates the structural model at depth. These computations therefore supply a realistic incoming S-wave and surface-wave wavefield which is used as input in the finite-difference computations.

Explicit finite difference schemes are used to simulate the propagation of seismic waves in the sedimentary basin. These schemes are based on the formulation of Korn and Stöckl (1982) for SH waves, and on the velocity-stress, finite difference method for P-SV waves (Virieux, 1986). The algorithms can

handle structural models containing a solid-liquid interface, and are numerically stable for materials with normal, as well as high values of Poisson's ratio. However, the numerical error increases with decreasing velocities, so it is usually bigger near the surface of the models. Therefore, in the P-SV case, a fourth-order approximation to the spatial differential operators is used for the upper part of the structural model (Levander, 1988). This offers the possibility to reduce the spatial sampling required to accurately model wave propagation. The finite difference operator in time is always of second order, since a fourth-order approximation would require too much computer memory.

A cause of error in the results of the hybrid technique can be the insufficient depth of the structural model described by the finite difference grid. When this insufficiency occurs, the signals are incomplete for receivers at large distances from the vertical grid lines where the incident wavefield is introduced into the finite difference computations. To deal with this problem, the lower artificial boundary of the finite difference grid is simply placed at greater depth. Moreover, to reduce the number of grid points in the vertical direction, the grid spacing is increased at depth. The number of grid points per wavelength in this deeper region of the structure is chosen large enough to prevent numerical errors.

Energy loss in unconsolidated sediments is an important process and should always be taken into account to prevent serious errors in seismic hazard estimations. In the finite difference computations, anelasticity is included by using the rheological model of the generalized Maxwell body (Emmerich and Korn, 1987; Emmerich, 1992; Fäh, 1992). This approach allows us to approximate the viscoelastic modulus by a low-order, rational function of frequency. This approximation of the viscoelastic modulus can account for a

constant quality factor over a certain frequency band. Replacement of all elastic moduli by viscoelastic ones, and transformation of the stress-strain relation into the time-domain, yields a formulation which can be handled with a finite difference algorithm (Emmerich and Korn, 1982).

The finite difference method has the disadvantage that limitations of computer memory require the introduction of artificial boundaries, which form the border of the finite difference grid in space. These boundaries are a severe problem in finite difference methods, since they can generate reflections of the waves impinging upon them from the interior of the grid. In this study, several methods for the prevention of these reflections are combined. Paraxial approximation of the wave equation (Clayton and Engquist, 1977) works well at the boundary limiting the structural model at depth. The two vertical boundaries at each side of the grid are chosen in relation to the grid spacing in the finite difference computations. In the case of a large grid spacing (50 m in the P-SV case; 25 m in the SH case), the method proposed by Smith (1974) reduces this contamination almost perfectly. Smith's method is only applied at the right boundary, whereas at the left boundary the paraxial approximation is chosen. With this technique, the contamination first appears at the right boundary having passed through the model two times. The disadvantage of Smith's boundary conditions is an increase in computer time by a factor of two. In the case of a small grid spacing (20 m in the P-SV case; 10 m in the SH case), Smith's boundary condition is too time-consuming. Then, the paraxial wave equation is also applied at the right artificial boundary. To improve the absorption at the artificial boundaries, regions of high absorption are introduced close to the boundaries. Since anelastic absorption is included in our numerical finite difference scheme, this approach requires no additional computer time. The quality factor Q has to be space dependent so that Q is decreasing linearly towards the artificial boundary. The gradient should not be

too steep to avoid reflections. With this method, the amplitude of the incoming wavefield is sufficiently well attenuated as long as the zone including damping is larger than the dominant wavelength. In the low-frequency part of the wavefield, the gradient of the quality factor close to the artificial boundary can produce reflections of the outgoing waves. Since the region of high absorption is characterized by the absence of low-velocity sediments, the grid spacing in the horizontal direction can be increased still having enough grid points per wavelength. This new grid spacing enlarge the geometrical extension of the region of high absorption and, therefore, reduces the steepness of the gradient of the quality factor.

Observations in Mexico City

From the geotechnical point of view, the valley of Mexico City can be divided into three zones (Figure 2): the hill zone, the transition zone, and the lake-bed zone. The hill zone is formed by alluvial and glacial deposits, and by lava flows. The transition zone is mainly composed of sandy and silty layers of alluvial origin. The surficial layers in the lake-bed zone consist mainly of clays. These deposits are poorly consolidated, with high water content and very low rigidity. The geometrical characteristics and mechanical properties are quite well-known from different borehole and laboratory tests. The mechanical properties exhibit a great variability. This surficial layer varies between 10 m and 70 m in thickness, where this thickness increases regularly towards the east (Suarez et al., 1987). The topmost layer is composed of compacted fill, and of the foundations for man-made structures (Chávez-Garcia and Bard, 1990). It is more resistant than the clay, and its thickness can be up to 10 m.

The clay layer is overlying the so-called "deep sediments" found below 10-70 m. These deeper deposits reach depths down to 700 m, where the uncertainty of the thickness of the deep sediments may be as large as a few hundred meters (e.g. Bard et al., 1988). The mechanical characteristics of the deep sediments are very poorly known; the topography of the bedrock interface has been estimated from boreholes and gravimetric data (Suarez et al., 1987). There are three outcrops of the basement: at Chapultepec, Peñon, and Cerro de la Estrella (Figure 2).

During the Michoacan earthquake, a strong motion network was operating in the valley of Mexico City (Mena et al., 1986). The positions of the stations are shown in Figure 2. Some of these were located in the lake-bed zone (SCT1, CDAO, CDAF), some in the hill zone (TACY, CUIP, CU01, CUMV), and one in the transition zone (SXVI). The observed displacements are shown in Figure 3. The records are corrected for the instrumental response and have been convolved with a high-pass Ormsby filter whose largest low-frequency cutoff is 0.10 Hz for the stations outside the lake-bed zone, and 0.07 Hz for those inside the lake-bed zone (Mena et al., 1986). These frequency limits do not influence our conclusions since the dominant energy in the synthetic signals is above these frequency limits.

Absolute time references are absent in the recorded signals. To estimate the relative times to an arbitrarly chosen zero-time, the signals have been shifted so that the long-period part of the vertical displacements are in phase (Campillo et al., 1988). This is justified since the long-period vertical displacements (Figure 2, label D/UP) have nearly identical waveforms and amplitudes at all stations. The time shifts have been given by Bard et al. (1988): CDAF (2.00 s), CDAO (35.75 s), SCT1 (26.00 s), TACY (40.00 s), CUIP (3.00 s) and CU01 (6.50 s). The time shifts for the stations SXVI and CUMV are not

given in the literature, and are here determined to be 4.50 s and 5.00 s, respectively.

The differences between the records in the lake-bed zone, and the records in the hill zone, reflect the differences at the sites. In the lake-bed zone (stations SCT1, CDAO and CDAF) the horizontal components of motion are the dominant ones. They have a larger high-frequency content than the corresponding vertical, or horizontal components recorded outside the lake-bed zone. The spectral peaks are in the interval between 0.2 Hz and 0.5 Hz.

Choice of the source and path models for the numerical modelling

The flat-layered structure, describing the path from the seismic source to the valley of Mexico City, is shown in Table 1. This model has been proposed by Campillo et al. (1989), and was deduced directly from refraction measurements in the Oaxaca, Southern Mexico region (Valdes et. al., 1986). The structural model is rather simple, in agreement with the resolving power of the available data. The depth of the Moho is about 45 km, and the upper five kilometers are composed of relative low-velocity material.

The epicenter of the Michoacan earthquake is close to the Pacific coastline. It is a typical intraplate subduction event, with a small dip angle and striking parallel to the Central-America trench. The rupture started in the north, and propagated through the zone of the 1981 Playa Azul earthquake with a low moment release (Eissler et al., 1986; Houston and Kanamori, 1986). It then ruptured an asperity in the south. Least-squares inversion of the Michoacan earthquake records, for the source time function, yielded three source pulses (Houston and Kanamori, 1986). The first two subevents have similar seismic moments ($1.1\text{-}1.7 \cdot 10^{21}$ N m) and durations (about 15 s); the moment of the third

is about 20 percent that of the first subevent, and has a duration of about 10 s (Eissler et al., 1986). The arrival time of the second event is shifted by 26 s, with respect to the first, and the location is about 80 km to the south-east of the first event. The third event occurred 21 s after the second one, and its position is about 40 km seawards of the second event. The Michoacan earthquake is characterized by high spectral amplitudes for periods between 2 and 5 s. Campillo et al. (1989) attribute the enhanced energy in the 2-to-5-second period range to the irregularity of the rupture propagation. They suggest that the rupture developed as a smooth crack towards the ocean.

For the computations presented here, an average source model for the 1985 Michoacan earthquake has been chosen. To keep the source model as simple as possible, we restrict the model first to a simple point source with a duration of 0 s. This allows us to study the behavior of the waves in the entire frequency band from 0.01 Hz to 1 Hz, with no a-priori assumptions about the frequency content of the source. This choice of a delta function will enhance high-frequency energy in parts of the computed ground motion. Therefore, for an easy qualitative comparison with the observed ground motion, we will only consider the displacement time series. The focal mechanism is the one proposed by Campillo et al. (1989), based on the results of Houston and Kanamori (1986) and Riedesel et al. (1986). The distance from the source to the valley of Mexico City is 400 km, the angle between the strike of the fault and the epicenter-station line is 220° (further on, referred to as the strike-receiver angle), the source depth is 10 km, the dip 15°, and the rake is 76°.

Due to uncertainties in the available models, only estimates of the strong ground motion in Mexico City can be given. Nevertheless, this modelling allows us to understand the main features of seismic wave propagation in the Mexico City valley as a consequence of strong earthquakes. One-dimensional

structural models for the Mexico City valley will be considered first, with the purpose of studying the one-dimensional response of the sedimentary cover with modal summation. The two-dimensional models that will then be considered, describe the cross-section from Chapultepec to Peñon across the sedimentary basin (for position see Figure 2). This cross-section is of particular interest since it intersects the area where extensive damage occurred in the strong earthquakes of 1957, 1979, and 1985. This area has been the subject of several theoretical studies (e.g. Sánchez-Sesma et al., 1988; Bard et al., 1988; Kawase and Aki, 1989). The final part is dedicated to the comparison between observed and synthetic seismograms.

One-dimensional structural models

The one-dimensional structural model used to describe the path from the source position to the sedimentary basin in Mexico City, is given in Table 1. Due to the large distance of Mexico City from the source, and the relatively low velocities of seismic waves in the upper crust, the signals are strongly dispersed (Figure 4). The simple, depth-limited structural model of Table 1 has only 15 modes in the frequency-phase velocity band being considered; the energy at frequencies below 0.2 Hz is limited to the fundamental mode, both for Love and Rayleigh waves.

In a second step of the one-dimensional modelling, the sedimentary cover that is present in the valley of Mexico City is included in our structural model. Two models are proposed. In the first, a surficial sedimentary layer of 400 m thickness replaces the upper 400 m of the model shown in Table 1. This layer represents the deep sediments. The second model is obtained from the previous one by replacing the upper 55 m of the deep sediments with a surficial clay

layer. The resulting 1D structure represents a one-dimensional model for the lake-bed zone. The values of the densities, body-wave velocities and quality factors of the layers are given in the captions of Figures 5 and 6, where the displacements obtained for both models are shown. The seismic source remains the same for all results shown in Figures 4, 5, and 6.

In passing from a model without a sedimentary layer (Figure 4), to a model with sediments (Figures 5 and 6), the arrival times and dispersion characteristics of the surface waves change. Group velocities decrease to values as low as 0.08 km/s for the model with the surficial clay layer. The main effect of the sedimentary cover on the fundamental mode is a strong dispersion, caused by the low-velocity surficial layer(s). The amplitudes of fundamental-mode Love and Rayleigh waves remain approximately the same for all three structural models, whereas for the high-frequency part of the wavefield, the amplitudes, the frequency content, and the arrival times are different. The amplitudes are larger for the models with a sedimentary cover. Due to the low shear-wave velocity of the clay layer, the high-frequency part (0.2-0.5 Hz) of the waves is concentrated in the horizontal components of motion (Figure 6). The vertical components of motion obtained for the different structural models are similar.

The seismograms obtained for the one-dimensional models of the Mexico City valley are of limited value for the interpretation of the observations in Mexico City; in fact, the surficial sedimentary layers are present only in the region surrounding Mexico City. In our results, this leads to unrealistically strong dispersion of the fundamental mode. On the other hand, these simple models show that the sedimentary cover can produce the observed concentration of the 0.2-0.5 Hz waves in the horizontal components. These models also explain the difference in amplitudes for receivers inside and outside the lake-bed zone, and

the almost unchanged form and amplitude of the vertical displacements (see Kawase and Aki (1989) for a review of the 1D results).

Before going into two-dimensional computations, we must first compare the results of modal summation and the hybrid technique for the simple case of a one-dimensional structural model. This comparison is necessary each time the hybrid technique is applied in a new region. The comparison allows us to establish control over the accuracy of the finite difference part of the computations, relative to: (1) the correct discretization of the structural model in space, (2) the efficiency of the absorbing, artificial boundaries, (3) the presence of all phases in the seismograms, and (4) the treatment of anelasticity. The comparison is performed for the same layered structural model which describes the path from the source position to the region where the finite difference method is applied (Table 1). It can be seen from Figure 7 that the results obtained with the hybrid technique and modal summation practically coincide. There are only small differences, which originate in the differences between the two computational techniques, and in the small reflections from the artificial boundaries.

Two-dimensional models: The Chapultepec-Peñon cross-section

Since the lake-bed zone is filled by the deep sediments and the clay layer, it is of interest to isolate the influence on the ground motion of these two layers. We first consider only the deep sediments. Due to uncertainties in the structural parameters, we consider different maximum thicknesses (400 m, 700 m) and two extreme values of the S-wave velocity (0.5 km/s, 1.0 km/s) of the sediments. In a further step, a low-velocity surficial clay layer is added to the structural model; this layer replaces the first tens of meters of the deep sediments. For all

computations, the source is the same impulsive point source (depth 10 km, dip=15°, rake=76°, angle strike-receiver=220°). The one-dimensional structural model, without the sediment and clay layer, describing the path from the source position to the valley of Mexico City is given in Table 1. This is the model used in the first portion of our hybrid computations, where the modal summation method is applied.

Effects of the deep sediments

The two-dimensional structure, modelling the Chapultepec-Peñon cross-section, is shown in Figure 8. The distances between the observation points and the source is in the range 400 to 412 km. The mesh size used in the finite difference grid is 25 m by 25 m for SH waves and 50 m by 50 m for P-SV waves.

The displacement time series, related to the receivers in Figure 8, are shown in Figure 9. In agreement with the observations in Mexico City during the Michoacan earthquake, our computational results show that the fundamental Rayleigh mode passes the sedimentary basin without significant change in amplitude and shape. The reason for this is the large wavelengths of the fundamental mode with respect to the spatial dimensions of the sedimentary basin. For the high-frequency part of the wavefield, however, there is a great spatial variability of ground motion within the sedimentary basin. Two adjacent observation points can have very different waveforms. In the sedimentary basin, the amplitudes of the transverse displacement dominates that for P-SV waves.

Due to the long duration of the incident wavefield, a superposition of different types of waves occurs. Therefore, it is difficult to distinguish different phases on the seismograms. In comparison with the results obtained for the 1D model

(Figure 4), the most important effect is the duration of the ground motion, which at some sites can be up to 40 s longer than in the 1D case. This effect is mainly caused by local surface waves and their reflections at the edges of the sedimentary basin, and is more pronounced for SH waves. This difference between the SH and P-SV case is due to the different dominant frequency content of the two wave types, which depends mainly on the source characteristics (e.g. depth, duration, rupture process). Local surface waves can only be a dominant phase in the seismograms if the incident wavefield has much energy in the frequency band of the excited local surface waves.

The uncertainty in ground motion predicted from numerical modelling can now be quantified by a parametric study. As the deep sediments are known very poorly, three different velocity models and thicknesses are considered. The first variant is characterized by a gradient in the material properties (shear wave velocities vary from 0.25 km/s at the surface to 0.6 km/s at the interface between sediments and bedrock). The second variant assumes a relatively high shear wave velocity for the deep sediments (β=1.0 km/s). The displacement time series for SH waves relative to the first and second variant, are shown in Figure 10A and B, respectively.

The model containing a gradient in the material properties is used to estimate the maximum possible effects caused by the deep sediments (Figure 10A). The effects are a strong amplification and the lateral propagation of local surface waves excited at the edges of the sedimentary basin. The model containing sediments with high S-wave velocities is used to estimate the minimum effects caused by the deep sediments (Figure 10B). Apart from a factor of about two in amplitude, there are no large variations between signals outside and inside the sedimentary basin. The difference in amplitudes can be explained by the

impedance contrast between bedrock and sediments. There is no significant excitation of local surface waves at the edges of the basin.

The maximum thickness of the deep sediments is increased to 700 m in the third and last variant. This deep basin causes the excitation of long-period local surface waves, which dominate the waveforms and increase duration (Figure 10C). Qualitatively, the results are the same as those discussed for the shallow sedimentary basin; however, in the deep basin local surface waves are mainly excited by the fundamental mode, while in the shallow basin higher modes are responsible for the generation of these local waves. This leads to very different shapes of the signals computed for the two structural models.

Effects of a clay layer

A surficial clay layer is now added to the structural model of the deep sediments (Figure 11). As indicated by the information available about the soil properties in Mexico City, the clay thickness increases gradually towards the east. Due to the very low shear-wave velocity of the clay (β=0.08 km/s), the mesh size used in the finite difference grid is 10 m by 10 m for SH waves and 20 m by 20 m for P-SV waves.

The displacement time series are shown in Figure 12. At the margin of the sedimentary basin, ground motion is determined mainly by the one-dimensional response of the uppermost clay layer. Within the basin, both for incident Love and Rayleigh waves, there is evidence of local surface waves which propagate in the clay layer. Local resonance effects lead to long duration and large amplitude codas; this phenomenon is most pronounced on the radial component, at distances of 409-410 km from the source. The resonance is excited by two distinct arrivals, the Lg waves and the fundamental Rayleigh

wave. Also for this model, the differences between the SH and P-SV case is due to the different frequency content of the two wave types. The vertical components of our synthetics, for frequencies below 0.5 Hz, are not significantly changed by the presence of the clay layer; this agrees with the recordings taken in Mexico City during the Michoacan earthquake.

A good representation of the amplification effects in sedimentary basins is given by the computation of spectral ratios between the signals obtained for the two-dimensional model (Figure 12), and the corresponding signals obtained for the one-dimensional model (Table 1). The results for the transverse and the radial components are shown in Figure 13, where these ratios are illustrated as a function of frequency and location along the section. The darker an area, the stronger are the amplifications that characterize the two-dimensional model with respect to the 1D case. The general distribution of the shaded areas can be related to the geometry of the structural model. Both the clay layer and the deeper sediments have an influence on ground motion observed at the surface. Their effects can be well separated, as is illustrated in the lower part of Figure 13, where the different features of the spectral ratios are interpreted and schematically represented. The greatest amplifications are caused by the clay layer, for frequencies close to the fundamental mode of resonance of a corresponding infinite flat layer. The maximum amplification with respect to the one-dimensional model is of the order of 30-50. This amplification factor coincides with the observed factors of up to 50 for the 1985 earthquake. At higher frequencies (above 0.8 Hz), there is also evidence for the excitation of the first higher mode of resonance for the clay layer. It must be mentioned that about the same spectral ratios are obtained if the 2D results are normalized to a specific reference ground motion observed outside the sedimentary basin.

At distances between 403 and 408 km from the source, and for frequencies above 0.5 Hz, the spectral ratios for the SH case are characterized by a relatively regular pattern of constructive and destructive interference. When considering the radial component of motion, more complicated features are seen (central part of Figure 13). These features are caused by resonances and by the fact that incident energy in certain frequency bands can be shifted from the vertical into the radial component of motion. These effects give rise to a series of dark lines in the spectral ratios for the radial component. For example, around 0.5 Hz and for distances between 403 and 408 km, spectral ratios reach values of up to 35.

Due to the variability of strong ground motion within the sedimentary basin, the poorly-known structure of the sedimentary basin in Mexico City, the simple source model, and the fact that none of the accelerometer stations are located on the cross-section studied, it is difficult to compare synthetic signals directly with observed strong ground motion. On the other hand, the two-dimensional model under study can be considered as sufficiently representative for the general geological situation in Mexico City. On observed records, an oscillation with a period of 2 to 5 s is superimposed on the fundamental modes (Figure 3). This feature has been interpreted as a source effect (Campillo et al., 1989) and is not present in our synthetic signals corresponding to a simple point source with 0 s duration. For the synthetic signals (Figure 12), the duration outside the sedimentary basin is about 90 s for P-SV waves and 60 s for SH motion, while within the sedimentary basin, the duration varies strongly and can have values of the order of 150 s in the P-SV case, and 120 s for SH waves. If we assume a seismic source that is composed of three subevents, as proposed by Houston and Kanamori (1986), the durations increase by about 45 s (Figure 14B) compared to those relative to a single event (Figure 14A). The durations and large amplitude codas are then in good agreement with observations in the

lake-bed zone. Some of the computed horizontal components of motion (Label L5.5 or R9.5 in Figure 14B) are very similar to the observed signals at station CDAO.

The model that we have used for the Mexico City area can explain the difference in amplitudes for receivers located inside and outside the lake-bed zone. The ratio between the computed, horizontal peak ground displacements inside and outside the lake-bed zone reaches values of the order of 5 to 7; about the same ratio is obtained for the observed ground motion.

In the central part of the sedimentary basin, the frequency content of the horizontal components of the computed ground motion agrees well with the observations, while the synthetic vertical displacements have too much energy for frequencies above 0.7 Hz. This can be accounted for in several ways, e.g. by the quality factor in the layered model (Table 1), or by the choice of the source time function. Assuming lower quality factors in the layered model (about half the values given in Table 1), or a source with finite duration (for example 3 s duration), will reduce the high-frequency content of the synthetic signals.

The applicability of the cross-section studied is confirmed by the fact that the spectral ratios obtained for the horizontal components of the synthetic seismograms can be very similar to the spectral ratios obtained from observations, as is shown in Figure 15. The maximum amplification factors, the shape of the spectral ratios, and the frequency bands at which amplification occurs, is explained by our numerical modelling. The two peaks in the spectral ratio for station CDAO can be attributed to the deep sediments (peak at about 0.8 Hz) and the surficial clay layer (peak at about 0.25 Hz). The spectral ratios for SH and P-SV waves are about the same. In the time domain, on the other hand, the local surface waves and resonance effects can only be a

dominant phase in the seismograms, if the incident wavefield has much energy in the frequency band of the excited surface waves and resonances.

Conclusions

The reasons for the damage caused by the Michoacan earthquake can be found in the special geological conditions of the valley of Mexico City. This valley consists mainly of two layers: the so-called deep sediments, and a surficial clay layer which is present in the lake-bed zone. By studying the one-dimensional response of these two layers with the modal summation method, it was possible to explain the difference in amplitudes between records for receivers inside and outside the lake-bed zone, also shown by Kawase and Aki (1989). These simple models show that the sedimentary cover produces the concentration of high-frequency waves (0.2-0.5 Hz) on the horizontal components of motion. One aspect that cannot be explained with one-dimensional models is the large amplitude coda of ground motion inside the lake-bed zone and the spectral ratios between signals observed inside and outside the lake-bed zone (Kawase and Aki, 1989). To achieve a realistic simulation of seismic ground motion in Mexico City, it is necessary to include source, path and local soil effects, to study SH and P-SV wave propagation, and to include also anelastic absorption. This simultaneous consideration of the different effects is the main advantage of the presented hybrid method, when compared with other techniques.

For realistic models of the sedimentary basin in Mexico City, the horizontal components of ground motion are mainly controlled by the response of the uppermost clay layer. Local surface waves and resonance effects lead to a long duration and a large amplitude coda of the signals inside the lake-bed zone.

Small variations of the geometry of the uppermost clay layer lead to very different ground motion in the horizontal components. Even in close neighboring stations it is possible to observe large differences in the shape, duration, and frequency content of the signals. The vertical components of our synthetics, for frequencies below 0.5 Hz, are not significantly changed by the presence of the clay layer; this agrees with the recordings taken in Mexico City during the Michoacan earthquake.

Spectral ratios that are computed for sites inside the sedimentary basin show that the clay layer, by interaction with the deep sediments, causes amplifications of the order of 30 to 50. This amplification factor agrees with those observed in the lake-bed zone. This value is larger than the one obtained by Bard et al. (1988) who computed amplification factors of up to 20 for vertically incident SH waves. Kawase and Aki (1989) attributed the long duration of ground motion and large amplitude coda observed in Mexico City to a strong interaction between the deep sediments and the surficial clay layer. They stated that the resonance frequencies of the two layers have to be almost the same to explain the long duration. Since the observed spectral ratios show the spectral peaks of the two layers at different frequencies, we suggest that the large amplitude coda observed at station CDAO is caused by a strong resonance effect in the laterally heterogeneous clay layer. Our numerical modelling also shows that for the explanation of the signals duration in the lake-bed zone, it is necessary to consider not only one-point source, but the energy contribution of the three subevents of the Michoacan earthquake.

The spectral properties of the seismic source control the frequency content of the incident wavefield; if the dominant energy is concentrated in the frequency band close to the resonance frequency of the clay layer or the deep sediments, local surface waves and resonance effects dominate the horizontal components

of motion within the sedimentary basin. For the same seismic source, SH and P-SV waves in general have their dominant energy in different frequency bands. In the numerical experiments, this consequently leads to differences in the ground motion: large excitation of local surface waves in the deep sediments for SH waves are not observed in the P-SV case. On the other hand, there are strong resonance effects in the clay layer for P-SV waves, that are less pronounced for SH waves.

The area of severe structural damage in Mexico City is characterized by increased thickness of the deep sediments and the laterally heterogeneous clay layer. Such geometries favor the excitation of local surface waves, which could be responsible for the observed distribution of damage. The large impedance contrast between the clay at the surface, and the deep sediments, causes strong resonance effects in the clay layer, which result in almost monochromatic wavetrains of long duration.

Acknowledgement

We would like to thank Fred Schwab, F. J. Sánchez-Sesma and the reviewers for their contribution to this research, and ENEA for allowing us the use of the IBM3090E computer at the ENEA INFO BOL Computer Center. This study has been made possible by the CNR contracts 90.02382.CT15, 91.02692.CT15, 90.01026.PF54 and 91.02550.PF54. This research has been carried out in the framework of the activities of the ILP Task Group II.4.

References

Alterman, Z. S. and F. C. Karal (1968). Propagation of elastic waves in layered media by finite difference methods, *Bull. Seism. Soc. Am.* **58**, 367-398.

Bard, P.-Y., M. Campillo, F.J. Chavez-Garcia, and F. J. Sánchez-Sesma (1988). The Mexico earthquake of September 19, 1985 - A theoretical investigation of large- and small-scale amplification effects in the Mexico City valley, *Earthquake Spectra* **4**, 609-633.

Ben-Menahem, A. and D. G. Harkrider (1964). Radiation patterns of seismic surface waves from buried dipolar point sources in a flat stratified Earth, *J. Geophys. Res.* **69**, 2605-2620.

Campillo, M., P.-Y. Bard, F. Nicollin, and F. J. Sánchez-Sesma (1988). The Mexico Earthquake of September 19, 1985 - The incident wavefield in Mexico City during the great Michoacan earthquake and its interaction with the deep basin, *Earthquake Spectra* **4**, 591-608.

Campillo, M., J.-C. Gariel, K. Aki, and F. J. Sánchez-Sesma (1989). Destructive strong ground motion in Mexico City: Source, path, and site effects during great 1985 Michaocan Earthquake, *Bull. Seism. Soc. Am.* **79**, 1718-1735.

Chávez-Garcia, F. J. and P.-Y. Bard (1990). Surface ground motion modifications by the presence of a thin resistant layer. Applications to Mexico City, *Proc. 9-th European Conference of Earthquake Engineering*, Sept. 11-16, 1990, Moscow, USSR, Vol. 4B, 37-46.

Clayton, R. and B. Engquist (1977). Absorbing boundary conditions for acoustic and elastic wave equations, *Bull. Seism. Soc. Am.* **67**, 1529-1540.

Eissler, H., L. Astiz, and H. Kanamori (1986). Tectonic setting and source parameters of the September 19, 1985 Michoacan, Mexico earthquake, *Geophys. Res. Lett.* **13**, 569-572.

Emmerich, H. and M. Korn (1987). Incorporation of attenuation into time-domain computations of seismic wave fields, *Geophysics* **52**, 1252-1264.

Emmerich, H. (1992). P-SV-wave propagation in a medium with local heterogeneities: a hybrid formulation and its application, *Geophys. J. Int.* **109**, 54-64.

Fäh, D., P. Suhadolc, and G. F. Panza (1990). Estimation of strong ground motion in laterally heterogenenous media: Modal summation - finite differences, *Proc. 9-th European Conference of Earthquake Engineering*, Sept. 11-16, 1990, Moscow, USSR, Vol. 4A, 100-109.

Fäh, D. (1992). *A hybrid technique for the estimation of strong ground motion in sedimentary basins*, Ph.D. thesis Nr. 9767, Swiss Federal Institute of Technology, Zurich.

Florsch, N., D. Fäh, P. Suhadolc, and G. F. Panza (1991). Complete synthetic seismograms for high-frequency multimode SH-waves, *Pageoph* **136**, 529-560.

Futterman, W. I. (1962). Dispersive body waves, *J. Geophys. Res.* **67**, 5279-5291.

Haskell, N. A. (1953). The dispersion of surface waves in multilayered media, *Bull. Seism. Soc. Am.* **43**, 17-34.

Houston, H. and H. Kanamori (1986). Source characteristics of the 1985 Michoacan, Mexico earthquake at periods of 1 to 30 seconds, *Geophys. Res. Lett.* **13**, 597-600.

Kawase, H. and K. Aki (1989). A study on the response of a soft basin for incident S, P, and Rayleigh waves with special reference to the long duration observed in Mexico City, *Bull. Seism. Soc. Am.* **79**, 1361-1382.

Knopoff, L. (1964). A matrix method for elastic wave problems, *Bull. Seism. Soc. Am.* **54**, 431-438.

Korn, M. and H. Stöckl (1982). Reflection and transmission of Love channel waves at coal seam discontinuities computed with a finite difference method, *J. Geophys.* **50**, 171-176.

Levander, A. R. (1988). Fourth-order finite-difference P-SV seismograms, *Geophysics* **53**, 1425-1436.

Levshin, A. L. (1985). Effects of lateral inhomogeneities on surface waves amplitude measurements, *Ann. Geophys.* **3**, 511-518.

Lysmer, J. and L. A. Drake (1972). A finite element method for seismology, in *Methods in Computational Physics*, B. A. Bolt, Editor, Vol. 11, Academic Press, New York, 181-216.

Mena, E., C. Carmona, R. Delgado, L. Alcántara, and O. Dominguez (1986). Catálogo de acelerogramas procesados del sismo del 19 de septiembre de 1985, parte I: Ciudad de México, *Series del Instituto de Ingenieria No. 497*, UNAM, México, D. F. México

Panza, G. F., F. A. Schwab, and L. Knopoff (1973). Multimode surface waves for selected focal mechanisms. I. Dip-slip sources on a vertical fault plane, *Geophys. J. R. astr. Soc.* **34**, 265-278.

Panza, G. F. (1985). Synthetic seismograms: The Rayleigh waves modal summation, *J. Geophysics* **58**, 125-145.

Panza, G. F. and P. Suhadolc (1987). Complete strong motion synthetics, in *Seismic Strong Motion Synthetics*, B. A. Bolt, Editor, Academic Press, Orlando, Computational Techniques **4**, 153-204.

Regan, J. and D. G. Harkrider (1989). Numerical modelling of SH Lg waves in and near continental margins, *Geophys. J. Int.* **98**, 107-130.

Riedesel, M. A., T. H. Jordan, A. F. Sheehan, and P. G. Silver (1986). Moment-tensor spectra of the 19 Sept. 85 and 21 Sept. 85 Michaocan, Mexico earthquakes, *Geophys. Res. Lett.* **13**, 609-612.

Sánchez-Sesma, F. J., S. Chávez-Pérez, M. Suárez, M. A. Bravo, and L. E. Pérez-Rocha (1988). The Mexico earthquake of September 19, 1985 - On the seismic response of the Valley of Mexico, *Earthquake Spectra* 4, 569-589.

Schwab, F. (1970). Surface-wave dispersion computations: Knopoff's method, *Bull. Seism. Soc. Am.* **60**, 1491-1520.

Schwab, F. and L. Knopoff (1972). Fast surface wave and free mode computations, in *Methods in Computational Physics*, B. A. Bolt, Editor, Vol. 11, Academic Press, New York, 87-180.

Singh, S. K. and M. Ordaz (1992). On the origin of lorg coda observed in the lake-bed strong-motion records of Mexico City. *Bull. Seism. Soc. Am.* in press.

Smith, W. D. (1974). A non-reflecting plane boundary for wave propagation problems, *J. Comp. Physics* **15**, 492-503.

Suarez, M., F. J. Sánchez-Sesma, M. A. Bravo, and J. Lermo (1987). Caracteristicas de los depósitos superficiales del Valle de México,

Memorias VII Congreso Nacional de Ingenieria Sismica, Querétaro, México, November 19-21, A61-A74.

Takeuchi, H. and M. Saito (1972). Seismic surface waves, in *Methods in Computational Physics*, B. A. Bolt, Editor, Vol. 11, Academic Press, New York, 217-295.

Thomson, W. T. (1950). Transmission of elastic waves through a stratified solid medium, *J. Appl. Phys.* **21**, 89-93.

Vaccari, F., S. Gregersen, M. Furlan, and G. F. Panza (1989). Synthetic seismograms in laterally heterogeneous, anelastic media by modal summation of P-SV-waves, *Geophys. J. Int.* **99**, 285-295.

Valdes, C. M., W. D. Mooney, S. K. Singh, R. P. Meyer, C. Lomnitz, J. H. Luetgert, C. E. Helsley, B. T. R. Lewis, and M. Mena (1986). Crustal structure of Oaxaca, Mexico, from seismic refraction measurements, *Bull. Seism. Soc. Am.* **76**, 547-563.

Virieux, J. (1986). P-SV wave propagation in heterogeneous media: Velocity-stress finite-difference method, *Geophysics* **51**, 889-901.

Layer	Thickness (km)	ρ (g/cm^3)	α (km/s)	β (km/s)	Q_α	Q_β
1	5.0	2.67	4.30	2.53	800	500
2	10.0	2.77	5.70	3.30	800	500
3	15.0	3.09	6.80	4.03	800	500
4	15.0	3.09	7.00	4.10	800	500
5	∞	3.30	8.20	4.82	800	500

Table 1. Numerical data for the schematic crustal model describing the path from the source in the Michoacan subduction zone, to Mexico City (Campillo et al., 1989).

Figure captions

Figure 1. Schematic geometry used in the hybrid method (see text).

Figure 2. Map of the area of Mexico City. On the map the locations of the strong motion accelerometer stations are shown; these stations were operating during the 1985 Michoacan event. The location of stations CU01 and CUIP are the same. The solid line indicates the cross-section, for which 2D modelling has been performed.

Figure 3. Horizontal and vertical components of displacement recorded in the valley of Mexico City (Mena et al., 1986). The NS-component of motion is denoted by D/NS, the EW-component by D/EW, and the vertical component by D/UP. In each column, the signals are normalized to the same peak displacement. The peak displacement is indicated in units of cm.

Figure 4. Transverse (left column), radial (middle column), and vertical displacements (right column) obtained for a point source (see text) in a 1D structural model (Table 1) at a distance of 400 km. All amplitudes are related to a source with seismic moment of 10^{-7} N m. The signals are normalized to the same peak displacement. The peak displacement is in units of cm. Each component is decomposed into different sets of modes (upper three traces for each component: modes 6-14, modes 1-5, fundamental mode FUND).

Figure 5. The same as in Figure 4, but replacing the first 400 m of the layered model (Table 1) with a surficial sedimentary layer, which represents the deep sediments (400 m thickness, ρ=2.0 g/cm^3, α=2.0 km/s, β=0.6 km/s, Q_α=100, and Q_β=50).

Figure 6. The same as in Figure 5, but now the model also contains a surficial clay layer (55 m thickness, ρ=1.3 g/cm^3, α=1.5 km/s, β=0.08 km/s, Q_α=50, and Q_β=25), which replaces the first 55 m of the sedimentary layer described in the caption of Figure 5.

Figure 7. Comparison between the displacement time series obtained with the mode summation method (Label MODE) and the hybrid technique (Label FD). All amplitudes are related to a source (see text) with seismic moment of 10^{-7} N m. In each column, the signals are normalized to the same peak displacement. The peak displacement is given in units of cm.
A) SH case: The distance between the source and the vertical grid lines, where the incident wavefield is introduced into the finite difference computations, is 400 km. The source-receiver distance is 412 km. The grid spacing is 25 m.
B) P-SV case (with the radial displacements on the left and the vertical ones on the right): The distance between the source and the vertical grid lines is 396.5 km. The source-receiver distance is 408.5 km. The grid spacing is 50 m.

Figure 8. Two-dimensional model related to the Chapultepec-Peñon cross-section. Only the part of the structure near the surface is shown, where the 2D model deviates from the plane-layered structural model.

Figure 9. Displacement time series for P-SV and SH waves at an array of receivers over cross-section Chapultepec-Peñon. All amplitudes are related to a source (see text) with seismic moment of 10^{-7} N m. In each column, the signals are normalized to the same peak displacement. The peak displacement is indicated in units of cm. The time scale is shifted by 90 s from the origin time (0 s in the figure is in fact 90 s from the origin time).

Figure 10. The same as in Figure 9 for the displacement time series for SH waves, assuming:
A) linear gradients in the material properties of the deep sediments: α=1.3-1.5 km/s, β=0.25-0.6 km/s, ρ=1.8 g/cm^3, Q_α=50-100, and Q_β=25-50.
B) relatively high wave velocities for the deep sediments: α=2.0 km/s, β=1.0 km/s, ρ=2.0 g/cm^3, Q_α=100, and Q_β=50.
C) a sedimentary basin with a maximum thickness of 700 m, and with material properties given in Figure 8.

Figure 11. Two-dimensional model related to the cross-section Chapultepec-Peñon, with a clay layer at the surface. Only the part of the structure near the surface is shown, where the 2D model deviates from the 1D layered structural model. In the lower part of the figure, an enlarged view of the clay layer is shown.

Figure 12. The same as in Figure 9 for the displacement time series, for cross-section Chapultepec-Peñon shown in Figure 11. The normalization factor of the time series is different from the one used in Figure 9.

Figure 13. Spectral ratios for the transverse and radial components of motion over the entire cross-section. The amplification effects are schematized and interpreted in the lower part of the figure. The step-like character of the spectral ratios clearly reflects the steps of the model in the finite difference computations.

Figure 14. Transverse (left column), radial (middle column), and vertical displacements (right column) obtained at three receivers within the sedimentary basin: at the western edge of the basin, 401.5 km from the source; in the centre of the basin, 405.5 km from the source; and at the eastern edge of the basin, 409.5 km from the source. The results of two computations are shown:

A) Synthetic displacements due to one point source.

B) Synthetic displacements due to three point sources, all located at a depth of 10 km and the same distance. The strike-receiver angle, dip and rake are 220°, 15°, 76°, respectively. The three point sources have different weights and time shifts (1.0, 1.0, 0.2 and 0 s, 26 s, 47 s). Weight 1 is given to a source with seismic moment of 10^{-7} N m.

Figure 15. Smoothed spectral ratios obtained for the synthetic seismograms (a) at 404 km and (b) at 409.5 km from the source, in comparison with the spectral ratios (c) of the horizontal components recorded at station SCT1 with respect to station TACY, and (d) of the horizontal components recorded at station CDAO with respect to station TACY.

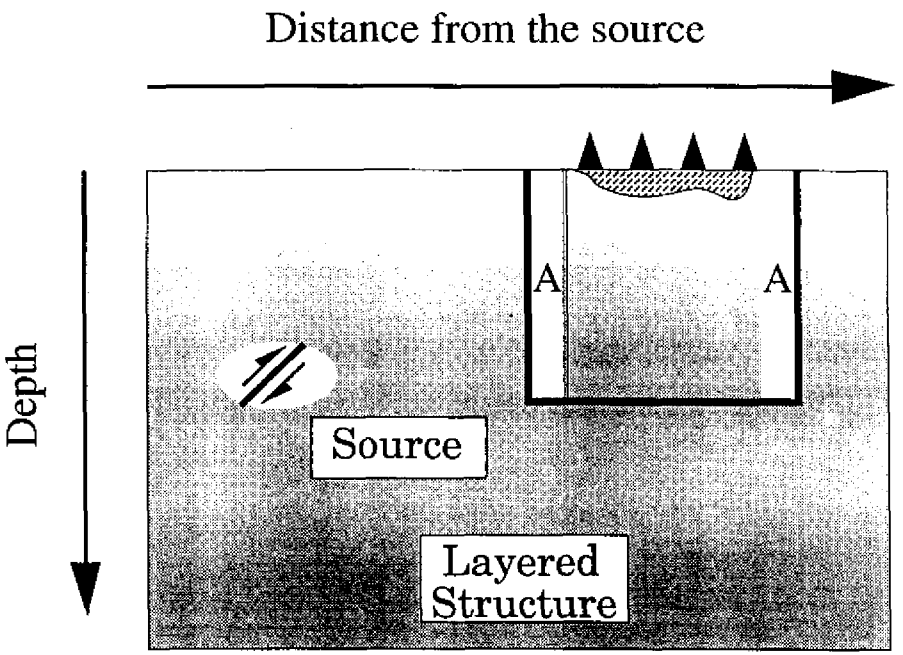

Artificial boundaries, limiting the finite-difference grid.

A Zone of high attenuation, where Q is decreasing linearly towards the artificial boundary.

Receiver

Adjacent grid lines, where the incoming wavefield is introduced into the FD-model. The wavefield has been computed with the mode summation technique. The two grid lines are transparent for backscattered waves (Alterman and Karal, 1968).

Fig.1

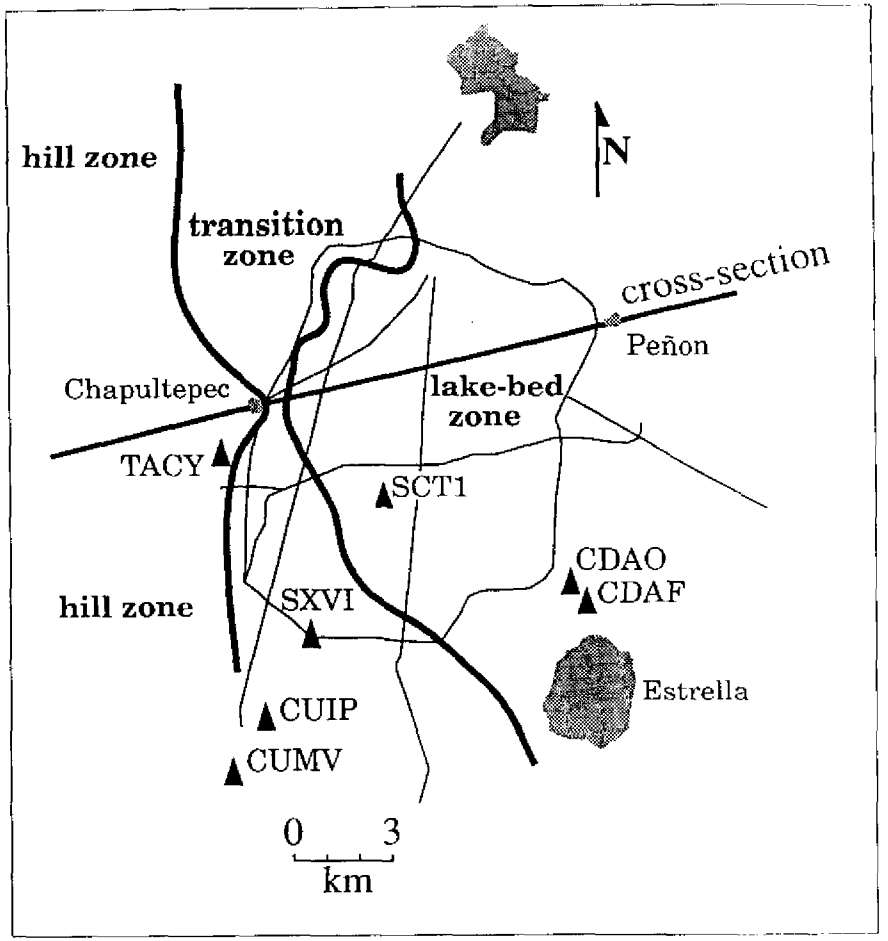
hill zone
transition zone
cross-section
Peñon
Chapultepec
lake-bed zone
TACY
SCT1
CDAO
CDAF
hill zone
SXVI
Estrella
CUIP
CUMV
N
0 3
km

Fig.2

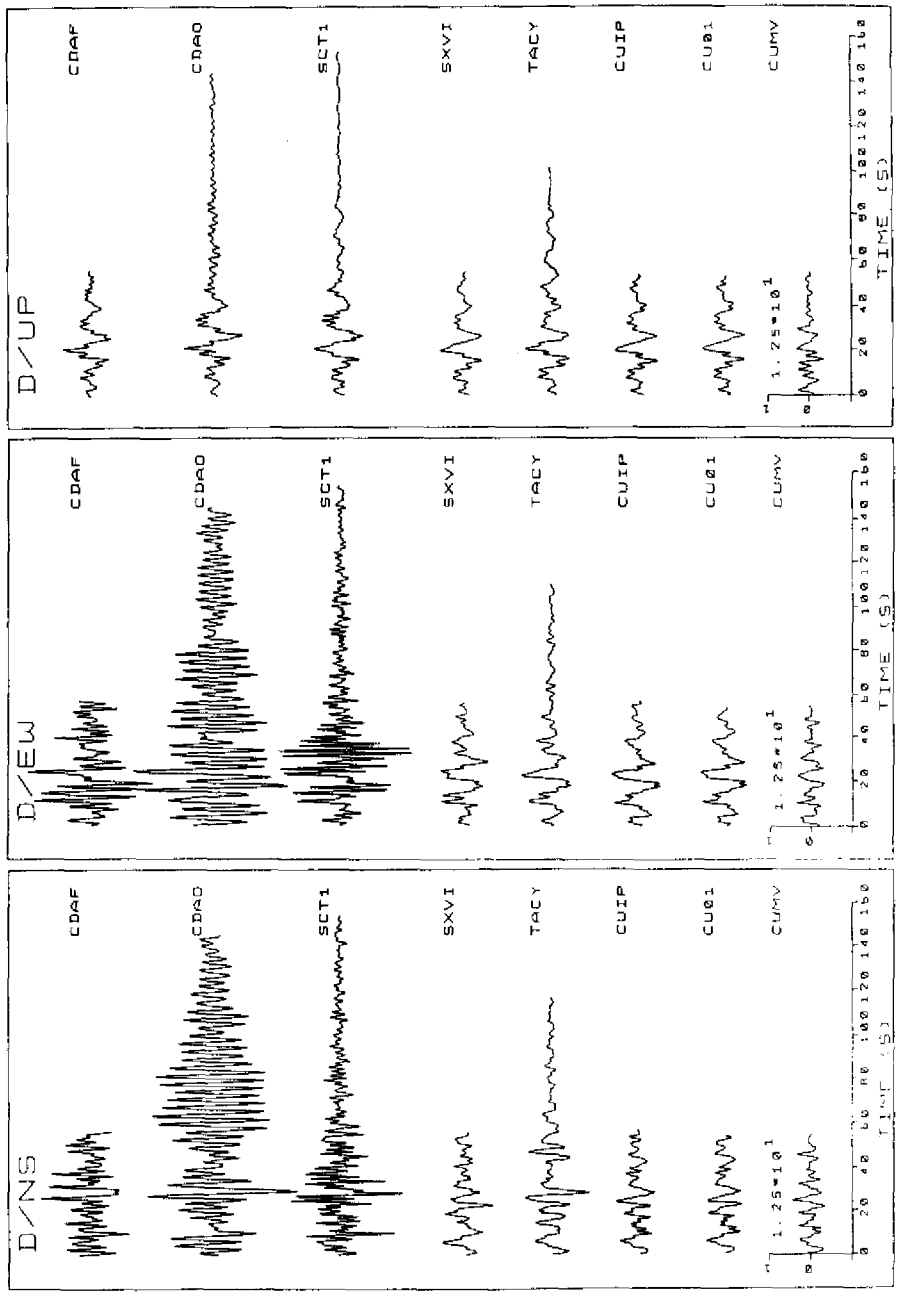
D/UP
D/EW
D/NS
CDAF
CDAO
SCT1
SXVI
TACY
CUIP
CUEI
CUMV
TIME (S)

Fig.3

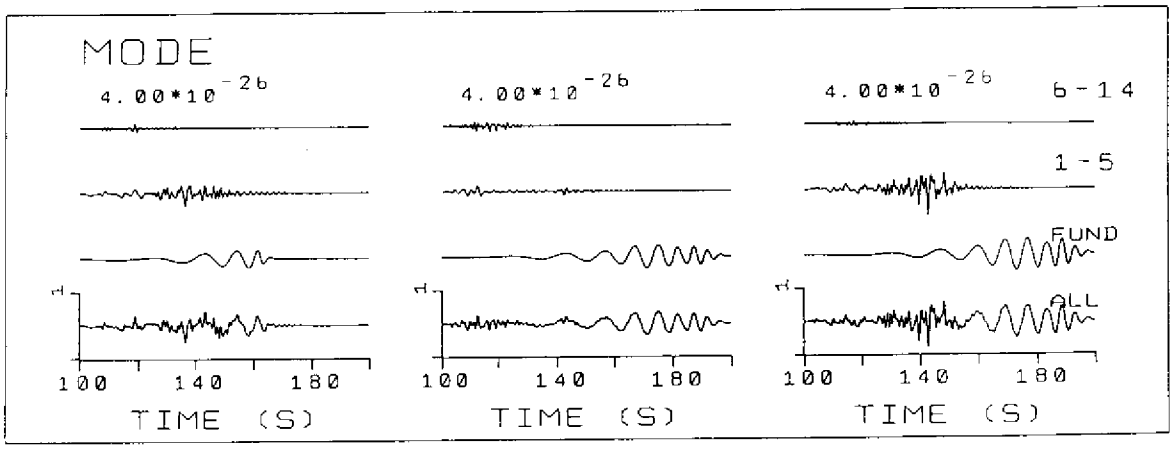
MODE
4.00*10^-26
4.00*10^-26
4.00*10^-26
6-14
1-5
FUND
ALL
100
140
180
TIME (S)
TIME (S)
TIME (S)

Fig.4

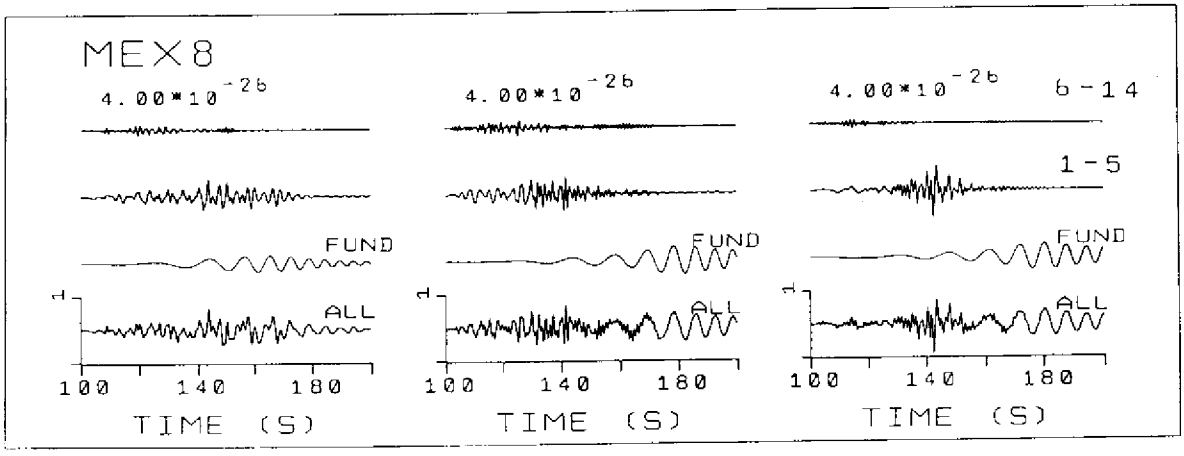
MEX8
4.00*10^-26
4.00*10^-26
4.00*10^-26
6-14
1-5
FUND
ALL
100
140
180
TIME (S)
TIME (S)
TIME (S)

Fig.5

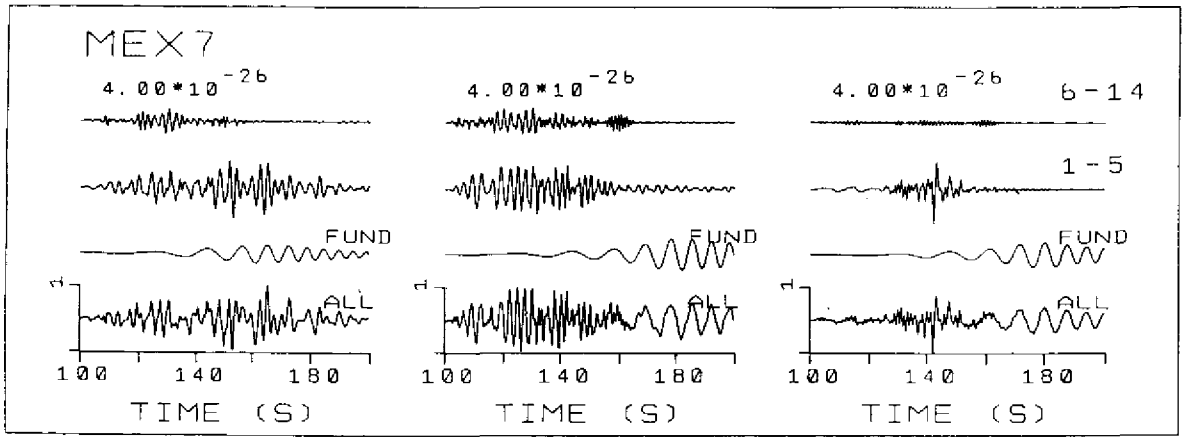
MEX7
4.00*10^-26
4.00*10^-26
4.00*10^-26
6-14
1-5
FUND
FUND
FUND
ALL
ALL
ALL
100
140
180
TIME (S)
TIME (S)
TIME (S)

Fig.6

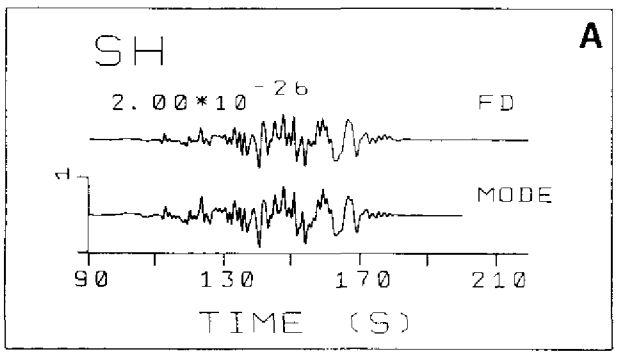
SH
A
2.00*10^-26
FD
MODE
90
130
170
210
TIME (S)

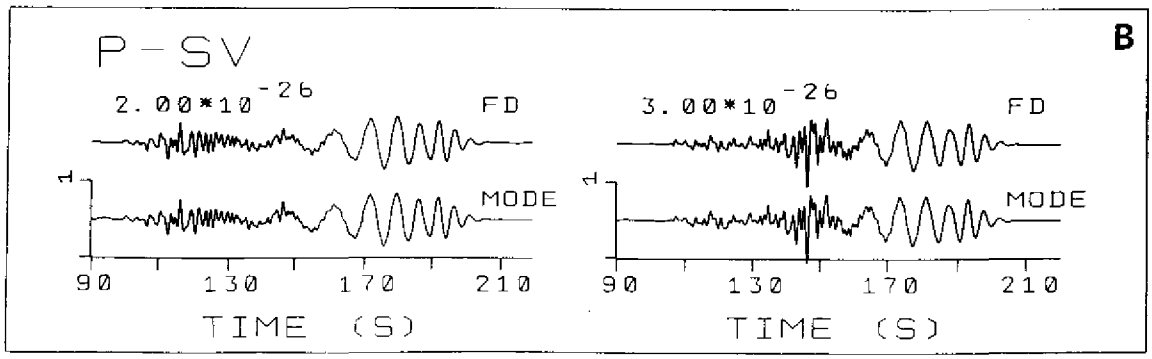
P-SV
B
2.00*10^-26
FD
MODE
3.00*10^-26
FD
MODE
90
130
170
210
TIME (S)
TIME (S)

Fig.7

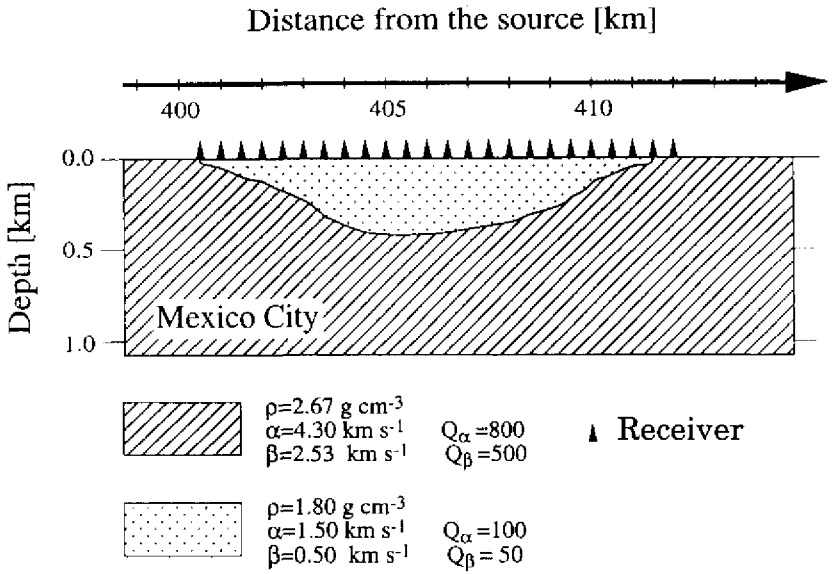
Distance from the source [km]
400
405
410
0.0
0.5
1.0
Depth [km]
Mexico City
ρ=2.67 g cm-3
α=4.30 km s-1
β=2.53 km s-1
Qα=800
Qβ=500
Receiver
ρ=1.80 g cm-3
α=1.50 km s-1
β=0.50 km s-1
Qα=100
Qβ=50

Fig.8

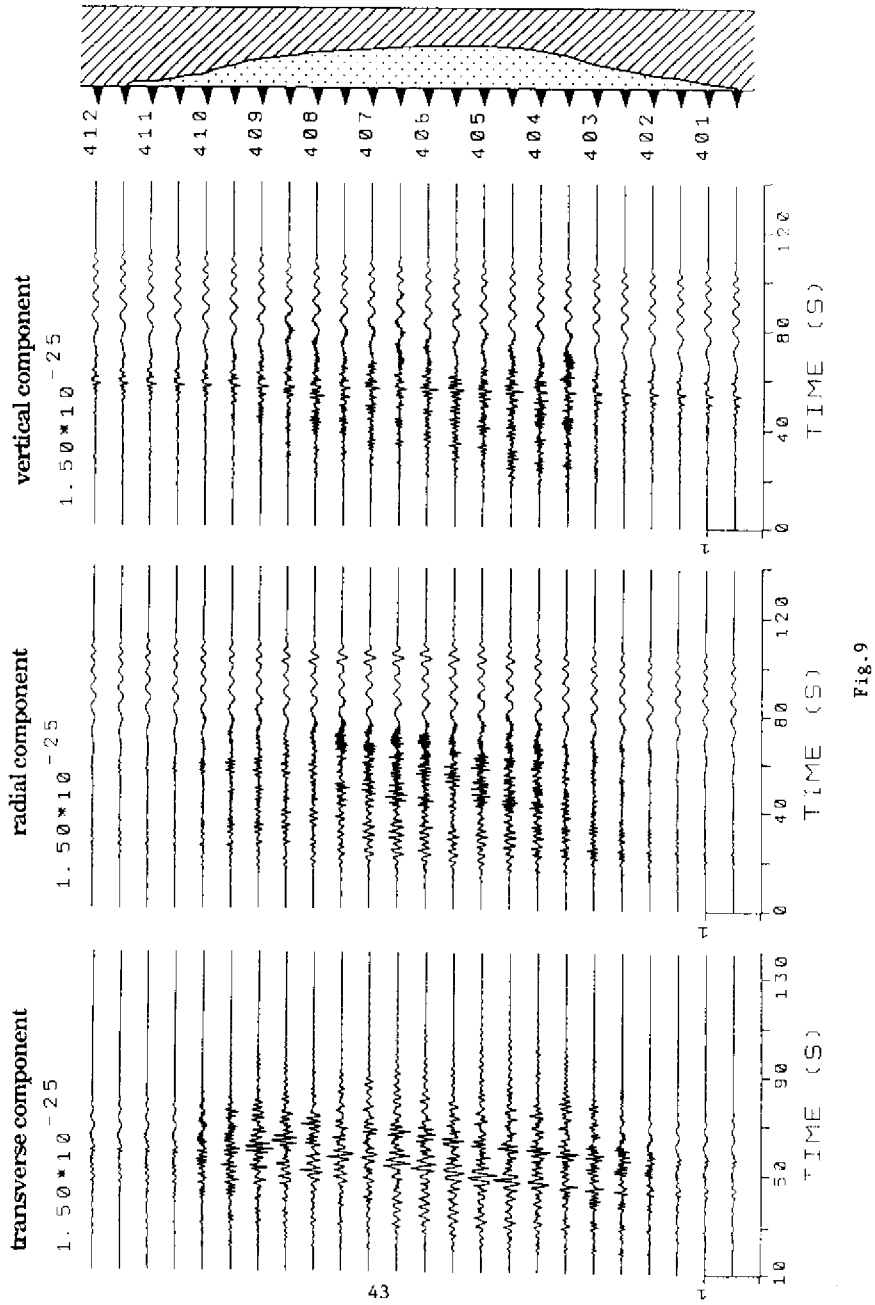
412
411
410
409
408
407
406
405
404
403
402
401
vertical component
1.50*10-25
radial component
1.50*10-25
transverse component
1.50*10-25
TIME (S)
TIME (S)
TIME (S)

Fig.9

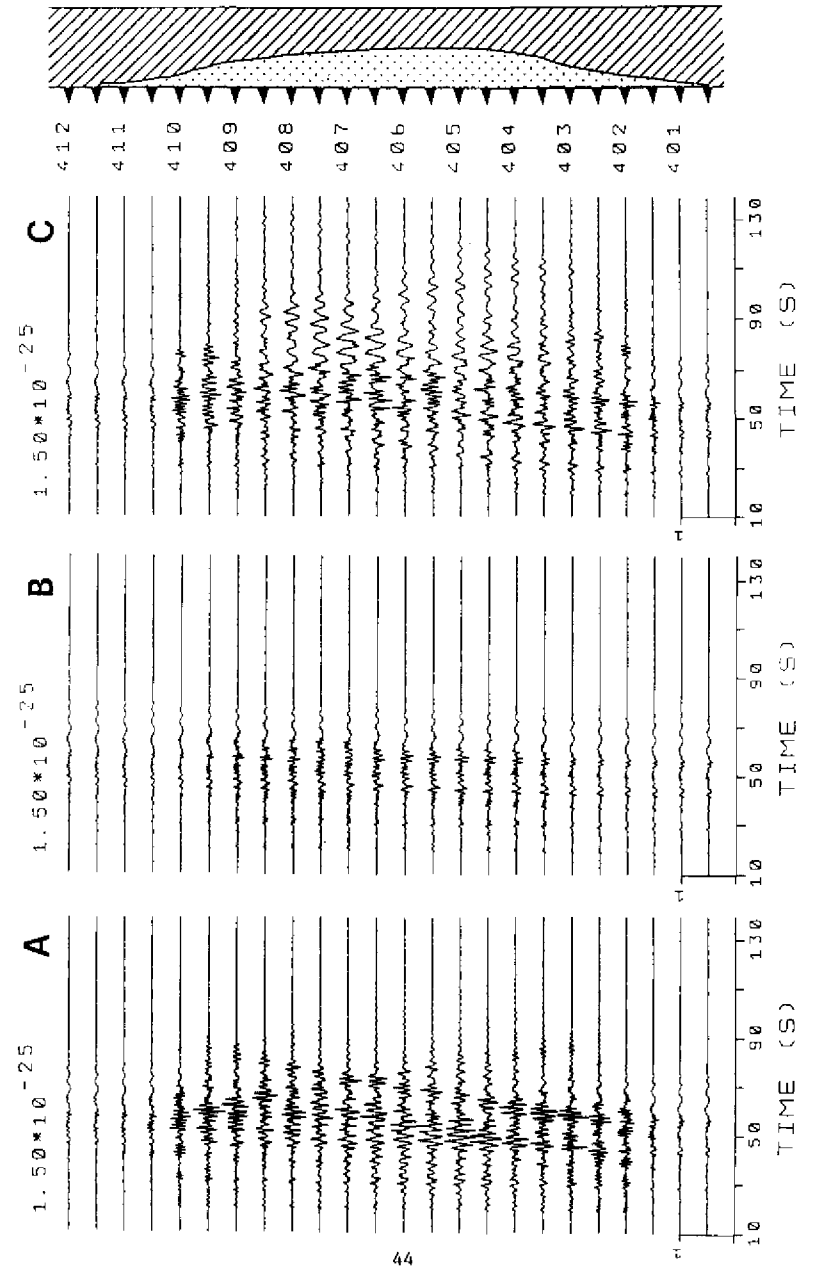
412
411
410
409
408
407
406
405
404
403
402
401
C
B
A
1.50*10-25
TIME (S)
10
50
90
130

Fig.10

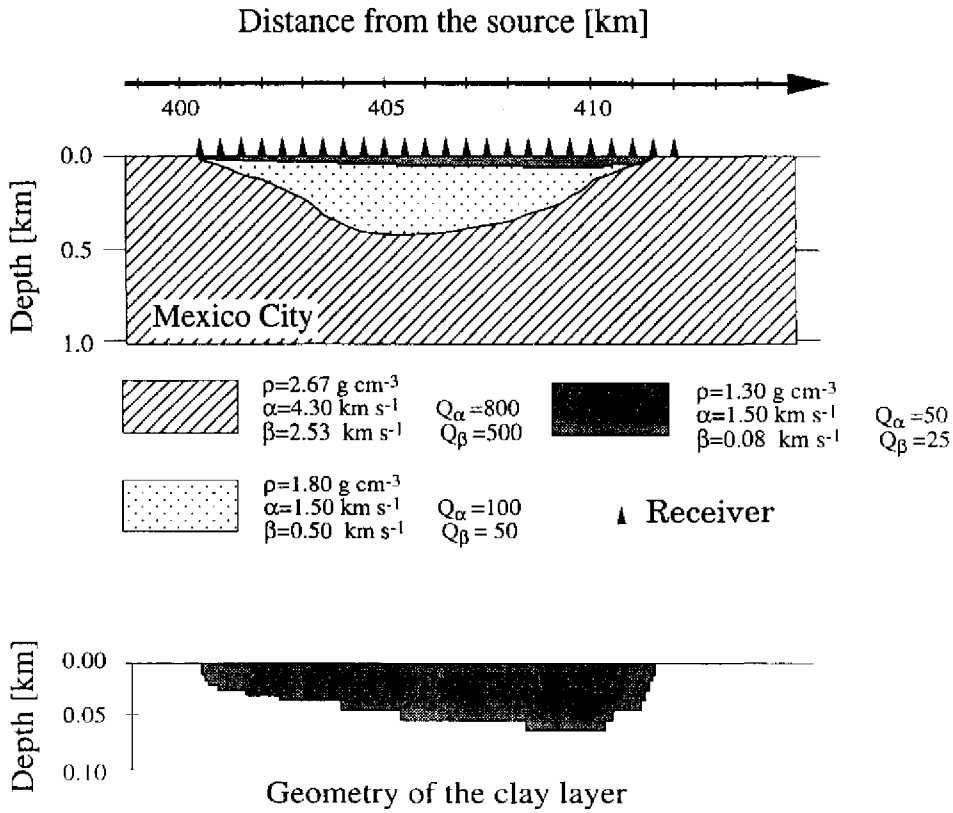
Distance from the source [km]
400
405
410
Depth [km]
0.0
0.5
1.0
Mexico City
ρ=2.67 g cm-3
α=4.30 km s-1
β=2.53 km s-1
Qα=800
Qβ=500
ρ=1.30 g cm-3
α=1.50 km s-1
β=0.08 km s-1
Qα=50
Qβ=25
ρ=1.80 g cm-3
α=1.50 km s-1
β=0.50 km s-1
Qα=100
Qβ=50
Receiver
Depth [km]
0.00
0.05
0.10
Geometry of the clay layer

Fig.11

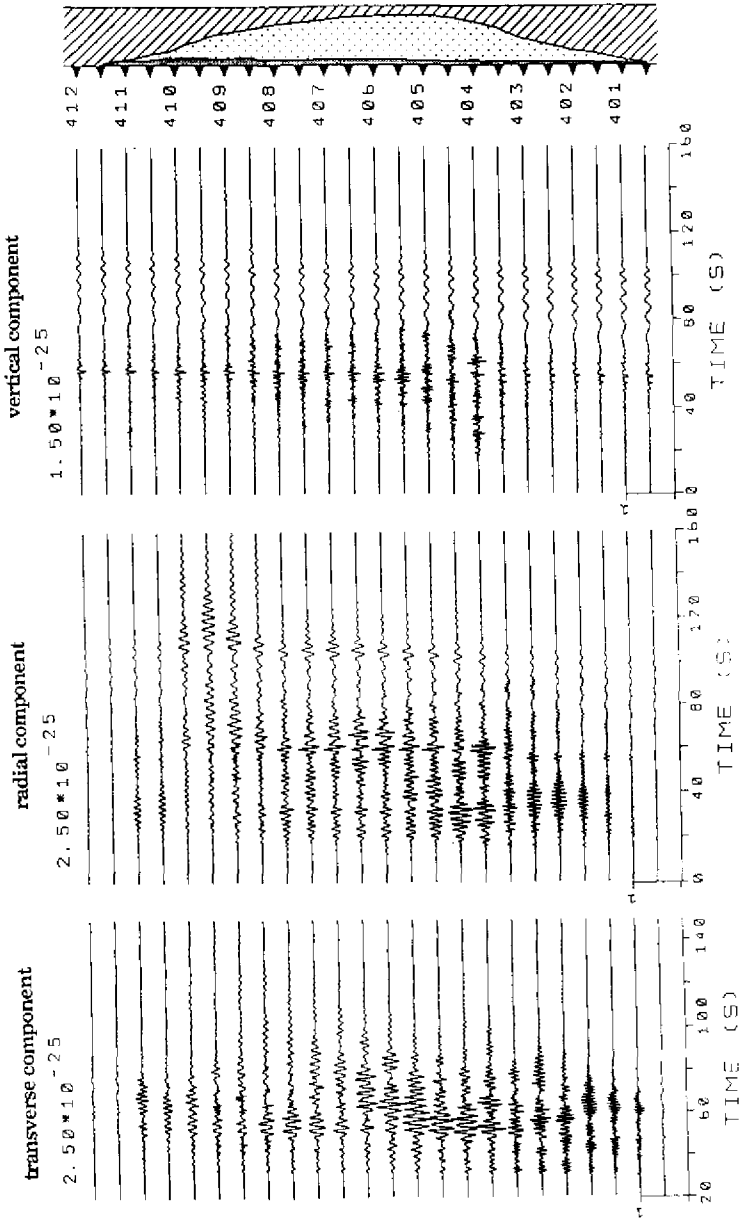
412
411
410
409
408
407
406
405
404
403
402
401
vertical component
1.50*10^-25
radial component
2.50*10^-25
transverse component
2.50*10^-25
TIME (S)
TIME (S)
TIME (S)

Fig.12

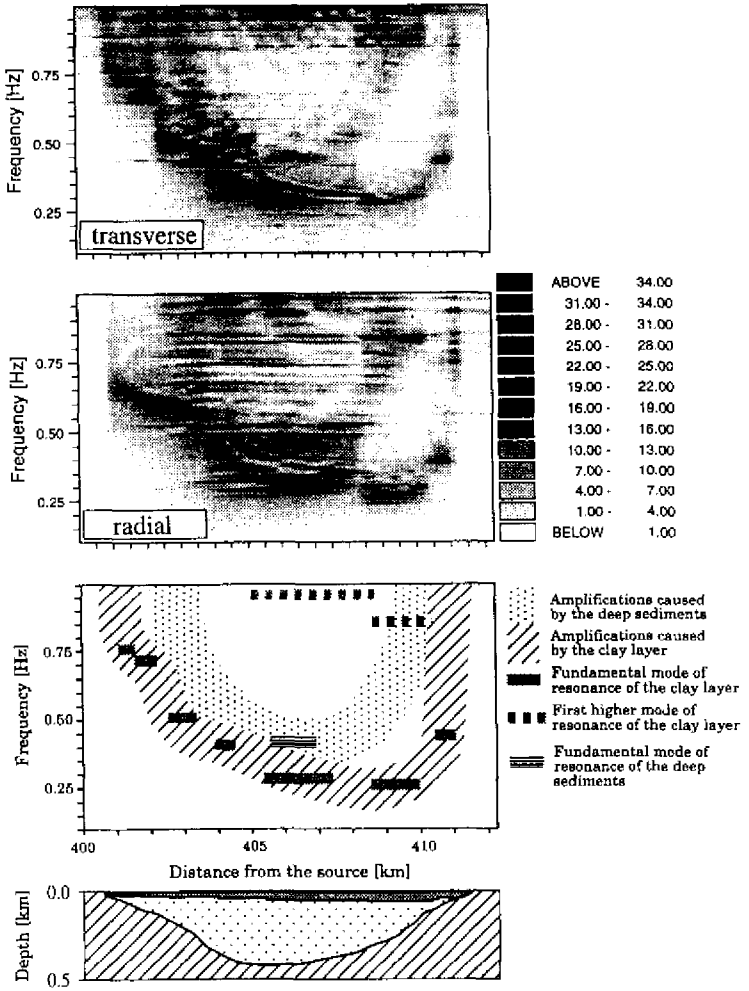
Frequency [Hz]
0.75
0.50
0.25
transverse
radial
ABOVE 34.00
31.00 - 34.00
28.00 - 31.00
25.00 - 28.00
22.00 - 25.00
19.00 - 22.00
16.00 - 19.00
13.00 - 16.00
10.00 - 13.00
7.00 - 10.00
4.00 - 7.00
1.00 - 4.00
BELOW 1.00
Amplifications caused by the deep sediments
Amplifications caused by the clay layer
Fundamental mode of resonance of the clay layer
First higher mode of resonance of the clay layer
Fundamental mode of resonance of the deep sediments
400
405
410
Distance from the source [km]
Depth [km]
0.0
0.5

Fig.13

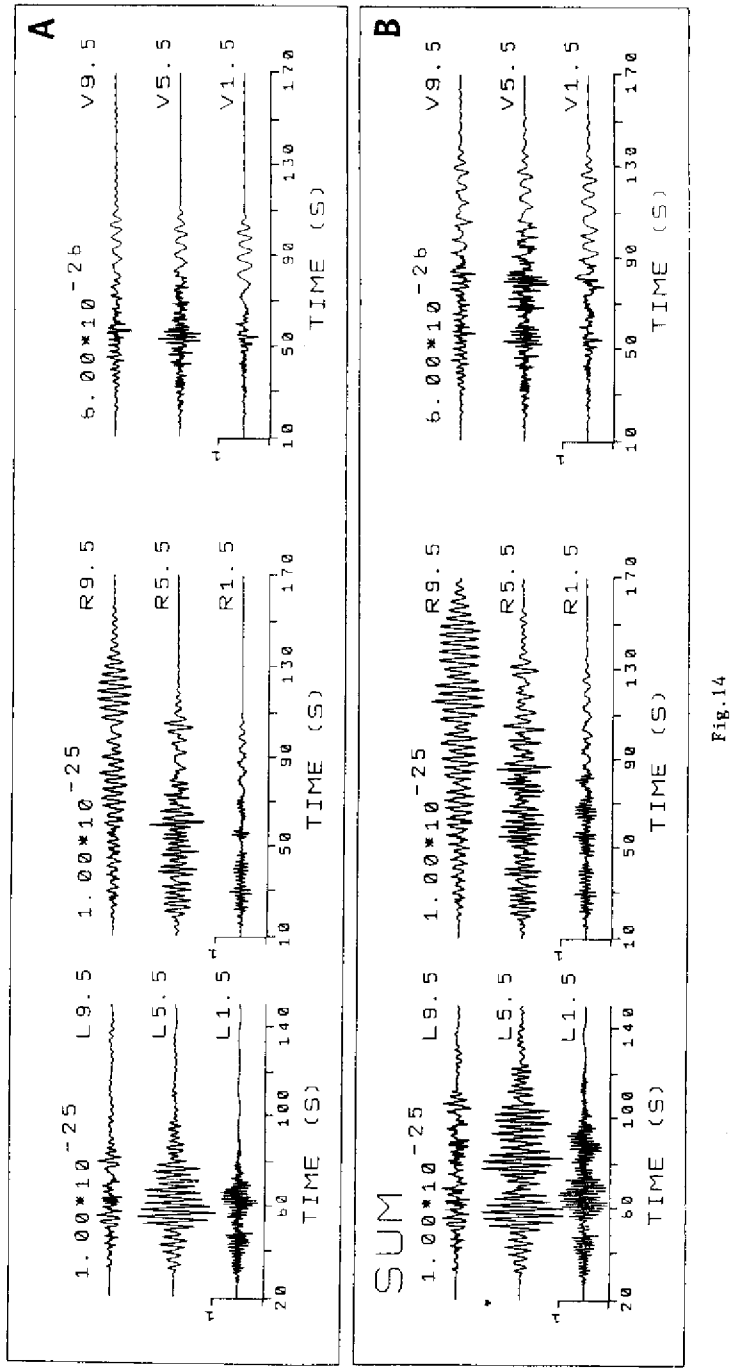
A
B
SUM
1.00*10-25
6.00*10-26
L9.5
L5.5
L1.5
R9.5
R5.5
R1.5
V9.5
V5.5
V1.5
TIME (S)

Fig.14

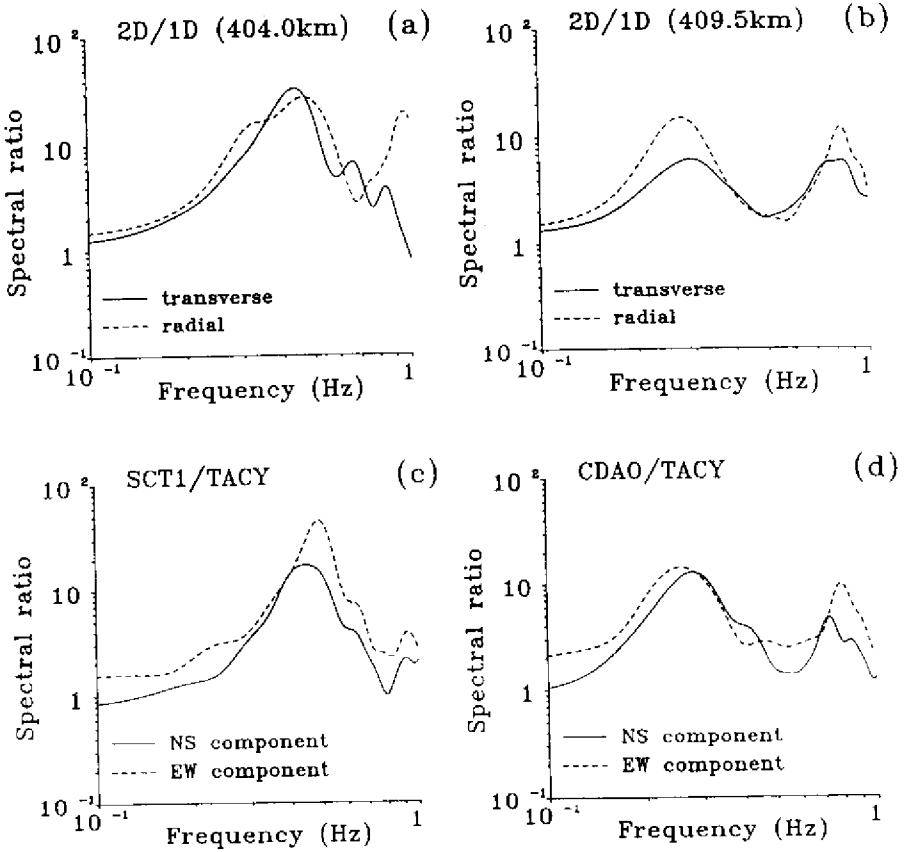
2D/1D (404.0km)
(a)
2D/1D (409.5km)
(b)
SCT1/TACY
(c)
CDAO/TACY
(d)
Spectral ratio
Frequency (Hz)
transverse
radial
NS component
EW component

Fig.15